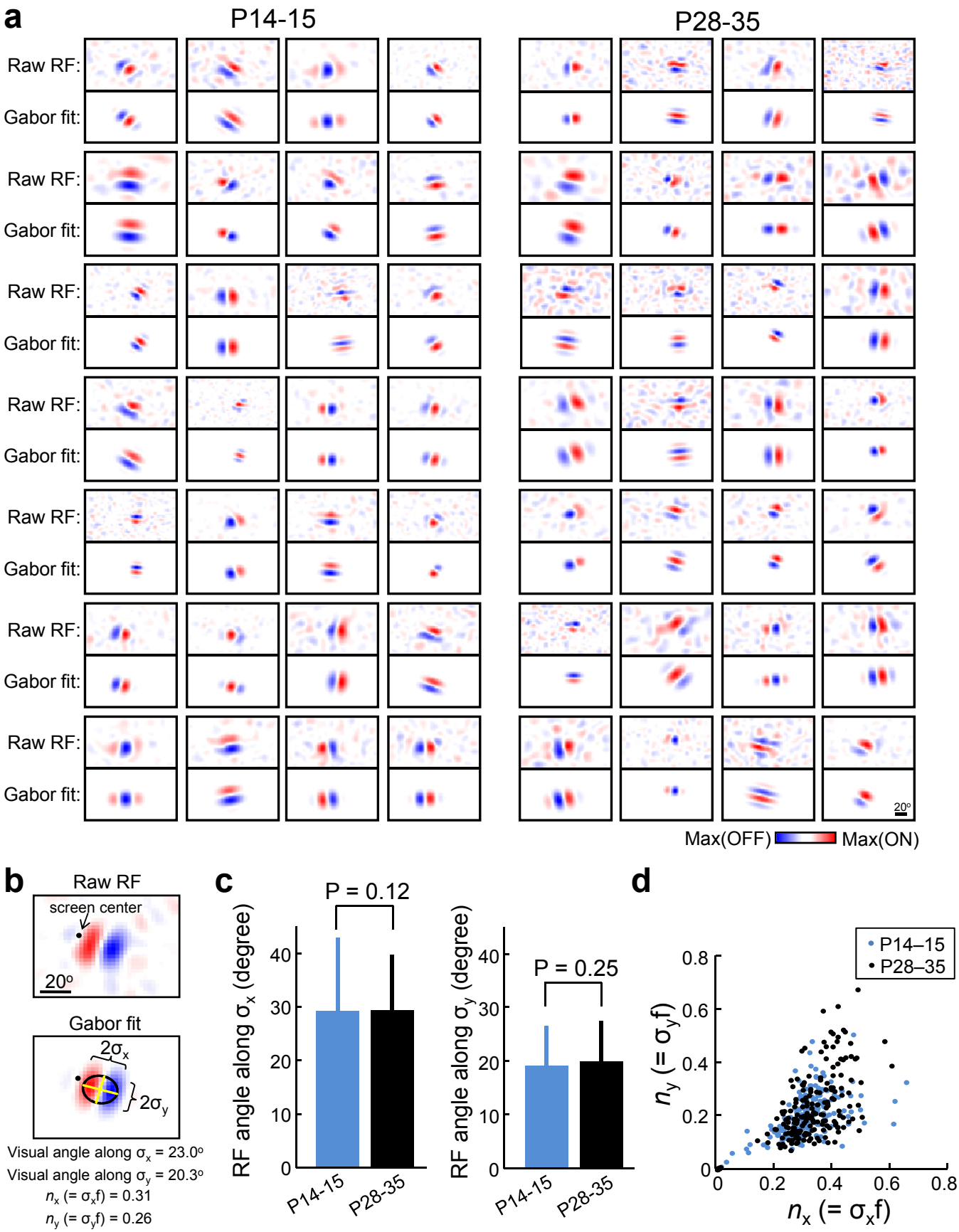

Supplementary Figure 1

Supplementary Figure 1. Quantification of RF parameters at eye-opening and with visual experience.

a, Example linear RFs at eye-opening (P14– 15) and in mature visual cortex obtained with reverse correlation. Below each RF is the corresponding Gabor fit (see Methods). **b,** Quantification of RF parameters. To obtain a measure of RF size, the visual angles subtended by the Gabor fit along the axes perpendicular (σ_x) or parallel (σ_y) to the direction of the cosine grating were calculated (see Methods). To quantify the shape of RFs, we used the dimensionless measures $n_x = \sigma_x f$ and $n_y = \sigma_y f$. These values express the size of the Gaussian envelope in terms of the wavelength of the underlying cosine grating. For instance, $n_x = 1$ indicates that the standard deviation of the Gaussian perpendicular to the grating is equal to half a cycle of the underlying cosine grating. **c,** Distributions of σ_x and σ_y were not different between immature and more mature V1 (mean visual angle along σ_x ± s.d., P14 – 15, 29.3 ± 13.6^o; P28 – 35, 29.4 ± 10.3^o; P = 0.12, rank-sum test; mean visual angle along σ_y ± s.d., P14 – 15, 19.1 ± 7.4^o; P28 – 35, 19.9 ± 7.7^o; P = 0.25, rank-sum test; error bars show s.d.). **d,** Distributions of n_x and n_y were not different between immature and more mature V1 (median n_x / n_y, P14 – 15, 0.31/0.20; P28 – 35, 0.32/0.20; P = 0.14/0.41, rank-sum test).

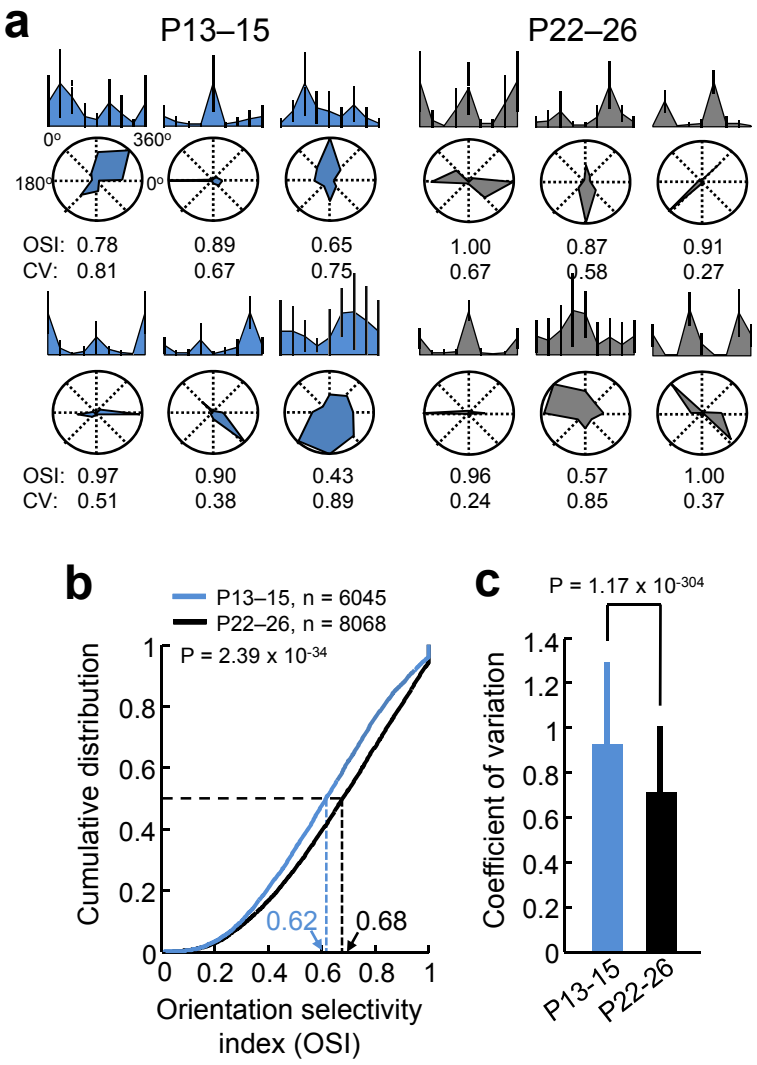

Supplementary Figure 2. Orientation selectivity and response reliability at eye-opening.

a, Examples of normalized tuning curves (inferred firing rate from calcium signals) and associated polar plots. OSI values were obtained from Fourier fitted tuning curves (see Methods). **b**, Cumulative distribution of orientation selectivity indices (OSI) at eye-opening and in more mature V1 (P13 – 15, median OSI 0.62 vs P 22 – 26, 0.68, P = 2.39 × 10-34, rank-sum test). **c**, Coefficient of variation (a measure of trial-to-trial variability, see Methods) of neuronal responses to the preferred grating direction was greater at eye-opening than in more mature V1 (mean CV ± s.d., P13 – 15,: 0.93 ± 0.36 vs P22 – 26, 0.71 ± 0.30, P=1.17 × 10-304, rank-sum test; error bars show s.d.). RF data acquired from 4 mice at P14 – 15, and 5 mice at P28 – 35.

Supplementary Figure 2

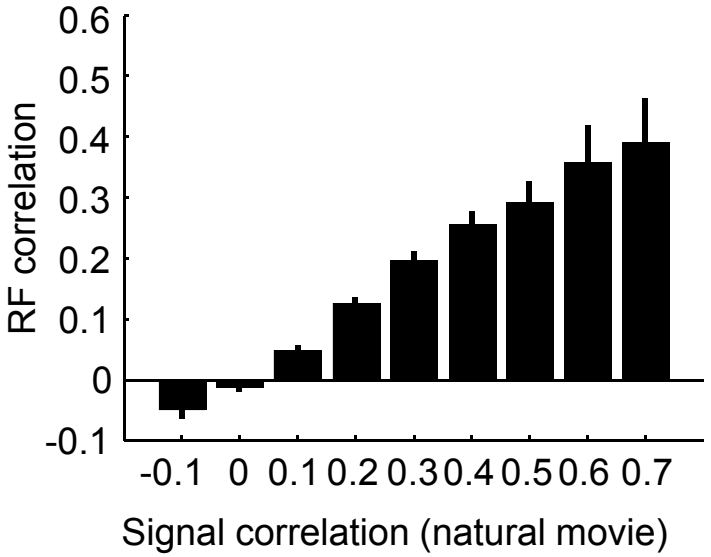

Supplementary Figure 3. Relationship between natural-movie signal correlation and RF correlation.

Neuronal pairs with higher signal correlations measured from responses to natural movies had higher linear RF correlations. Error bars show s.e.m. Correlation values were binned, with ranges from -0.15 to -0.05, from -0.05 to 0.05, etc.

Supplementary Figure 3

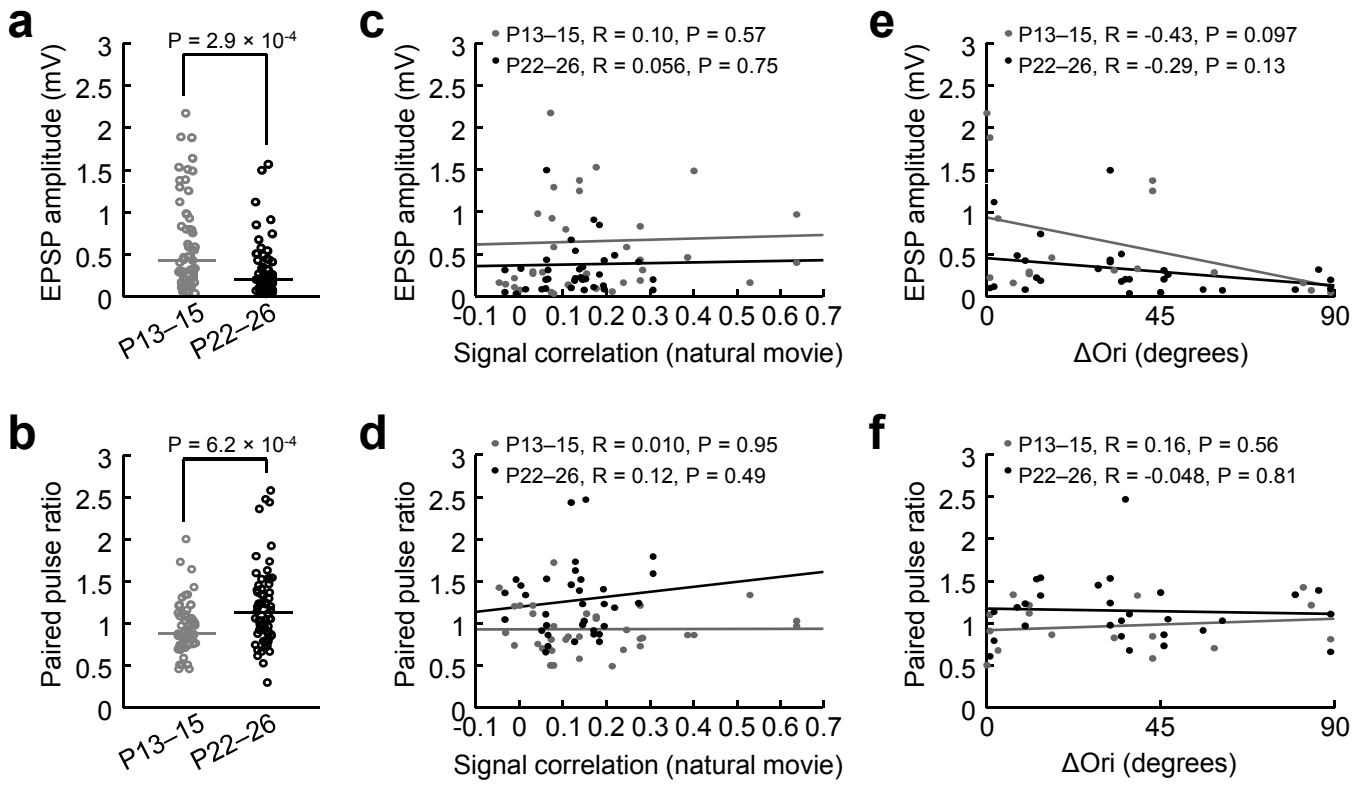

Supplementary Figure 4. Relationship between natural-movie signal correlation or difference in preferred orientation and EPSP amplitude and paired-pulse ratio.

a, EPSP amplitudes between L2/3 pyramidal neurons were significantly larger at eye-opening than in more mature V1 (median EPSP amplitude, P13 – 15, 0.41 mV VS P22 – 26, 0.20 mV, P = 2.9 × 10-4, rank-sum test). **b**, Paired-pulse ratios between L2/3 pyramidal neurons were significantly lower at eye-opening than in more mature V1 (median PPR, P13 – 15, 0.87, VS P22 – 26, 1.13, P = 6.2 × 10-4, rank-sum test). **c**, **d**, There was no correlation between EPSP amplitudes (**c**) or paired-pulse ratio (**d**) and signal correlation at either eye-opening or in more mature V1 (P > 0.5). **e**, There was a non-significant trend of decreasing EPSP amplitude with increase in difference in preferred orientation in both age groups (P13 – 15, R = -0.43, P = 0.097; P22 – 26, R = -0.29, P = 0.13). **f**, There was no significant correlation between PPR and difference in preferred orientation (P > 0.5 for both groups).

Supplementary Figure 4